

# Low Sonic-Boom Design Using Numerical Optimization

Yoshikazu MAKINO and Hirotohi KUBOTA  
*University of Tokyo, Tokyo 113, Japan*

Takashi AOYAMA and Toshiyuki IWAMIYA  
*National Aerospace Laboratory, Tokyo 182, Japan*

## Abstract

A study of the aerodynamic design for the reduction of sonic-boom is conducted by combining a 3-dimensional Euler CFD code with a least-square optimization technique. This method can consider a nonlinear and a 3-dimensional effects of aircraft which cannot be considered by previous low-boom design methods based on linear theory. The fuselage geometry of a low-boom aircraft designed by linear theory is modified by this design method in order to minimize the pressure discrepancies between a target low-boom pressure signature and a calculated signature. It is shown that the sonic-boom intensity of the aircraft designed by this method is smaller than that designed by linear theory. The results of the study indicate that this method is a useful tool for low-boom design.

## I. Introduction

The sonic-boom caused by supersonic overland flight is one of the biggest environmental problems for the supersonic transport (SST). A lot of prediction methods for the sonic-boom have been already developed. Whitham<sup>1</sup> presents a modified linear theory called the 'F-function method'. The F-function is calculated from the equivalent area distribution which is composed of two basic contributions: the actual area of the configuration and the equivalent area due to the distribution of lift. Thomas<sup>2</sup> presents a computational method to extrapolate a near-field pressure signature out to the far-field, which is called the 'Waveform parameter method'. This method needs a near-field pressure signature as input data. Computational fluid dynamics (CFD) is one of the most suitable approaches to simulate the near-field pressure signature because it is applicable to a case which includes strong shock waves. In this study, a finite difference code is used to predict the near-field pressure signature.

Many kinds of methods to reduce the sonic-boom intensity have been presented. Seebass and George<sup>3</sup> show the area distribution which minimized the sonic-boom intensity. However, the area distribution has an extremely blunt nose shape which produces large drag. Darden<sup>4</sup> modifies this minimization method in order to reduce the drag by controlling the bluntness of the area distribution near the nose. In this article, the sonic-boom intensity of a low-boom configuration is predicted in order to point out limitations of the upper low-boom design methods based on linear theory, and a new low-boom design method which combines a 3-dimensional Euler CFD code with a least-square optimization technique<sup>5</sup> is presented.

## II. Previous Low-Boom Design Method

Figure 1 shows the concept of Darden's low-boom design. This method is based on the F-function method. The F-function is defined by several parameters and each parameter has an influence on the shape of the ground pressure signature or the sonic-boom intensity. Figure 2 shows three types of low-boom pressure signatures: a flat-top type, a ramp type, and a hybrid type pressure signature. Darden's low-boom design method can consider the first two types. A flat-top type pressure signature is generated when the parameter B in Fig. 1 is 0.0, and a peaky type pressure signature is generated when B has a positive value. The F-function shown in Fig. 1 has a spiked part in the nose region and the parameter  $y_f$  is the width of the spiked part. This parameter controls the nose bluntness of the aircraft. The aircraft has a blunt nose when  $y_f$  is small.

Figure 3 shows the low-boom aircraft configuration<sup>6</sup> designed by Darden's method. The dimensions of this aircraft are: aircraft length ( $L=300$  [feet]), weight (700,000 [lb]) and wing planform area (12,000 [feet<sup>2</sup>]). Flight conditions are: design Mach number ( $M=1.4$ ), design lift coefficient ( $C_L=0.116$ ) and flight altitude (42,000 [feet]). The wing planform is first determined by a supersonic theory for drag reduction, and the wing is

warped to reduce induced drag. The fuselage geometry is determined by the solution of boom minimization. The configuration has an equivalent area distribution which is designed to generate a flat-top type pressure signature on the ground by Darden's theory. The initial peak pressure level estimated by linear theory is 0.87 [psf]. The value of the parameter  $y_f/L$  for this configuration is set at 0.00001, which means a blunt nose. Figure 4 shows the equivalent area distributions of this low-boom configuration. The equivalent area distribution ('volume+lift') is composed of two basic contributions: the actual area of the configuration ('volume'), and the equivalent area due to the distribution of lift ('lift'). This figure indicate that this low-boom aircraft is accurately designed in accordance with Darden's low-boom design method.

Figure 5 shows the predicted ground pressure signature for the low-boom configuration compared with the design signature obtained in our previous study<sup>7</sup>. In this figure, the predicted pressure signature shows a flat-top shape in the front part and the initial peak pressure level is about 1.0 [psf], which is about the same as the initial design value of 0.87 [psf]. However, there are some discrepancies between the predicted ground pressure signature and the design signature, and the maximum pressure level in the predicted signature is about 2.0 [psf]. One reason for these discrepancies is the nonlinear effect of the shock waves generated from the aircraft because the F-function method is based on linear theory. Another reason is the 3-dimensional effect of the aircraft because the 3-dimensional configurations are converted to their equivalent axisymmetrical body in the F-function method. Therefore, a low-boom design method which can consider the nonlinear and the 3-dimensional effects of aircraft is needed.

### III. New Low-Boom Design Method

In this article, a new low-boom design method by coupling the 3-dimensional Euler CFD code and a least-square optimization technique is presented. The fuselage geometry of an aircraft is modified axisymmetrically in order to minimize the discrepancies between the calculated near-field pressure signature and the target signature. The axial distribution of radial perturbation is defined by a B-spline curve controlled by K points, whose radial coordinates  $\delta_k$  are design variables in the optimization process. The optimization method used in this study is based on a least-square technique. The differences between the target and baseline pressures are reduced by adding perturbations to the baseline fuselage geometry iteratively. The object function to be minimized through the optimization is:

$$J = \sum_{i=1}^I \left( P_{ti} - P_{bi} - \sum_{k=1}^K \frac{\partial P_i}{\partial \delta_k} \delta_k \right)^2 \Delta S_i \quad (1)$$

where K is the number of design variables. The quantity  $\partial P_i / \partial \delta_k$  is the response of the flowfield to the small radial perturbation  $\delta_k$ ,  $P_{ti}$  and  $P_{bi}$  are the target and baseline pressures in the pressure signature at point  $i$  ( $i=1 \sim I$ ), respectively, and  $\Delta S_i$  is the length of the  $i$ th element of the pressure signature. The unknown  $\delta_k$  is to be determined by a least-square method. The target pressure signature is given in the near-field of the aircraft. This target near-field pressure signature is determined so that the ground pressure signature extrapolated from it by the waveform parameter method becomes the target low-boom ground pressure signature.

### IV. Design Results

The initial low-boom configuration shown in Fig. 3 is modified in order to generate a flat-top type pressure signature on the ground, shown in Fig. 5 (dashed line). The target pressure signature is given at the distance of  $H/L=6.0$  below the aircraft. The number of design variables represented by K, which is the number of controlling points for a B-spline curve, equals 8. In the design process, most of the computation time is consumed in the CFD analysis, because it is needed to calculate the flowfield K+1 times in one optimization cycle to find flowfield responses to the geometry perturbations.

Figure 6 shows the optimized near-field pressure signature with the target and baseline pressure signatures. The figure shows that the optimized pressure signature is flatter than the baseline signature. Figure 7 shows the ground pressure signatures extrapolated from the near-field pressure signatures in Fig. 6. Comparing the baseline pressure signature with the optimized one, the maximum peak pressure level drops from 2.1 [psf] to 1.2 [psf]. The sonic-boom intensities of these ground pressure signatures evaluated by dB(A) are shown in the figure. The rise time of the shock overpressure in the ground pressure signature is predicted from the following empirical relation<sup>8</sup> between the rise time  $\Delta T_R$ , and the shock overpressure  $\Delta p$ .

$$\log \Delta T_R = A_1 \log \Delta p + A_2 \quad (A_1 = -0.920, A_2 = 2.23) \quad (2)$$

The sonic-boom intensities of the target and optimized ground pressure signatures evaluated by dB(A) are about the same, although there are a few discrepancies between these signatures as shown in Fig. 7. The sonic-boom intensity for the optimized low-boom configuration is about 2 dB(A) smaller than that for the baseline configuration.

The optimized fuselage shown in Fig. 8 becomes wider in the rear part than the baseline because a strong expansion wave must be generated from the aircraft tail to reduce the pressure peak due to the shocks from the leading edge of the outer wing. Figure 9 shows the equivalent area distribution of the optimized configuration. The optimized distribution (Volume+Lift) is different from the designed distribution (Design). This discrepancy means a correction by considering the nonlinear and the 3-dimensional effects of the aircraft.

## V. Conclusions

The boom intensity of a low-boom configuration designed by linear theory is predicted by the 3-dimensional Euler CFD code and the waveform parameter method. It is indicated that there are some discrepancies between the predicted ground pressure signature and the designed low-boom pressure signature because of the nonlinear and 3-dimensional effects, although the initial peak pressure level of the low-boom configuration is about the same as the initial design value.

A new low-boom design method which combines the 3-dimensional Euler CFD code with the least-square optimization technique is presented in order to consider the nonlinear effect of the flow-field and the 3-dimensional effect of the aircraft. The sonic-boom intensity of the low-boom configuration designed by linear theory is reduced by this method. Therefore, it is indicated that this method is a useful tool for low-boom design.

## Acknowledgement

The authors express their sincere gratitude to Kawasaki Heavy Industries, Ltd. for providing the low-boom aircraft configuration data.

## REFERENCES

- <sup>1</sup> Whitham, G.B., Communications in Pure and Applied Mathematics, Vol.V, 1952.
- <sup>2</sup> Thomas, C.L., NASA TN D-6832, 1972.
- <sup>3</sup> Seebass,R. and George,A.R., Journal of the Acoustical Society of America, Vol.51, No.2 (Part.3), 1972.
- <sup>4</sup> Darden, C.M., NASA TP-1348, 1979.
- <sup>5</sup> Lee, D.K. and Eyi, S., Journal of Aircraft, Vol.29, No.6, 1992.
- <sup>6</sup> Yoshida, K., AIAA paper 94-0052, 1994.
- <sup>7</sup> Makino, Y., Sugiura, T., Watanuki, T., Kubota, H., Aoyama, T. and Iwamiya, T., AIAA paper 97-2213, 1997.
- <sup>8</sup> Darden, C.M. and Shields, E.W., AIAA paper 93-2942, 1993.

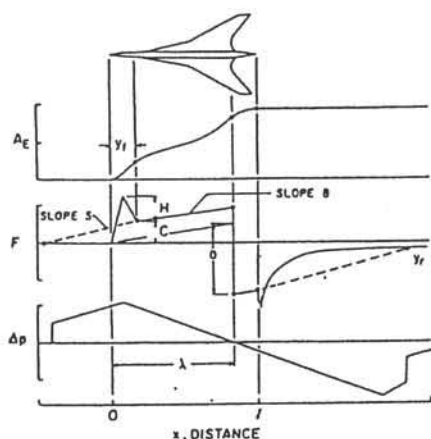


Fig. 1 Concept of low-boom design<sup>4</sup>.

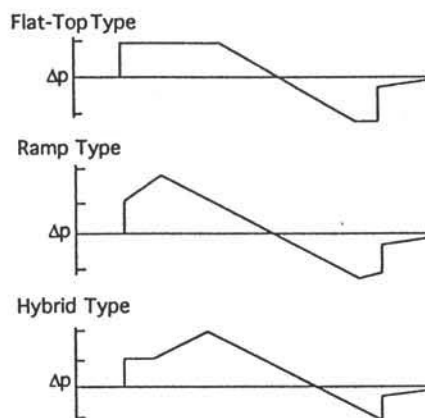


Fig. 2 Low-boom pressure signatures.

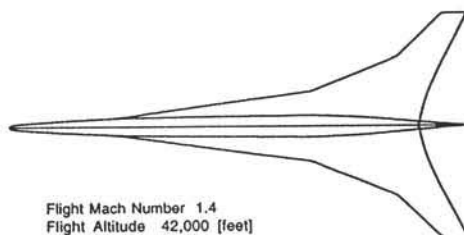


Fig. 3 Low-boom configuration.

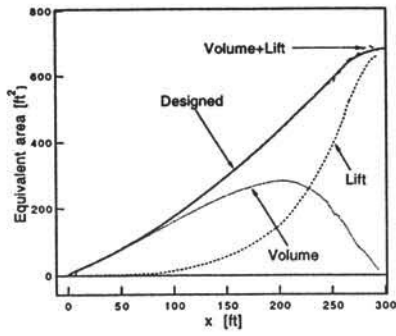


Fig. 4 Equivalent area distributions.

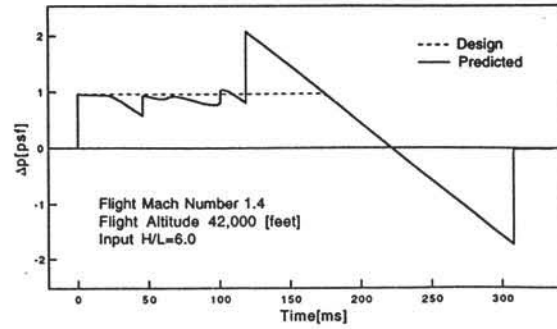


Fig. 5 Ground pressure signature.

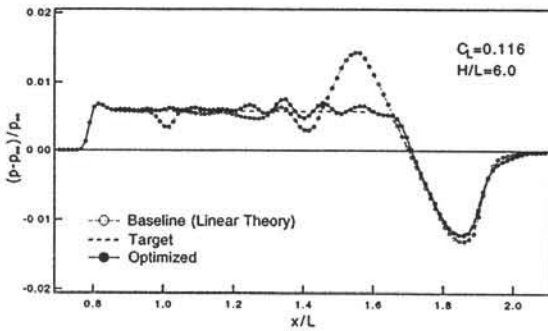


Fig. 6 Optimized near-field pressure signature.

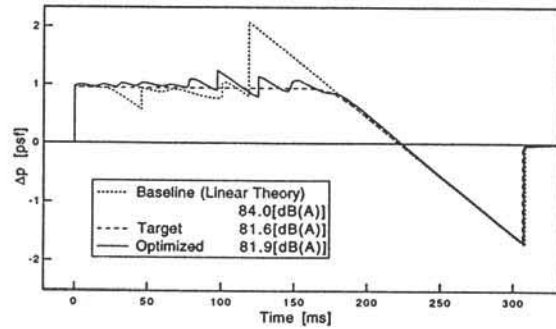


Fig. 7 Optimized ground pressure signature.

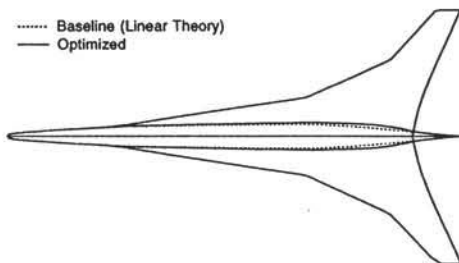


Fig. 8 Optimized fuselage geometry.

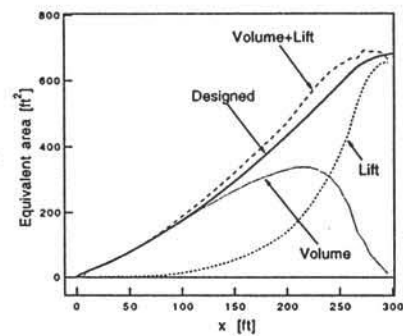


Fig. 9 Optimized equivalent area distributions.